



# How does the choice of the input hydrograph affect reservoir and dam design?

Dina Pirone, Andrea D’Aniello, Luigi Cimorelli and Domenico Pianese

Department of Civil, Architectural and Environmental Engineering, University of Naples Federico II, via Claudio 21, 80125 Napoli, Italy

*Correspondence to:* Dina Pirone (dina.pirone@unina.it)

**Abstract:** Reservoir and dam design requires a detailed understanding of the entire input hydrograph rather than relying solely on peak discharge estimates. Input hydrographs are essential both for verification purposes to evaluate the peak attenuation capacity of the reservoir and for design purposes to define reservoir height, its volume and outlet structures. However, no universal guidelines exist for selecting the input hydrograph, leaving designers to navigate conflicting methodologies often without clear evidence of the advantages and drawbacks of different hydrographs. As a result, the choice of the input hydrograph is typically based on local regulations, introducing subjectivity and potential inconsistencies. This study investigates how sensitive reservoir and dam design is to the choice of the input hydrograph by quantifying the differences in reservoir key parameters, such as the maximum outflow discharge, maximum storable volume, and peak reduction effect. The analysis compares the results of the most commonly used input hydrographs and continuous time series routing. The study highlights the advantages and potential limitations of commonly used input hydrographs, particularly regarding their ability to represent hydrological conditions of the time series accurately. The findings of this study aim to offer a more conscious approach to hydrograph selection, potentially reducing subjectivity and improving the robustness of reservoir and dam design practices. Finally, the study seeks to address computational challenges associated with reservoir routing by identifying efficient yet reliable hydrograph options.

## 1 Introduction

Designing hydraulic infrastructures or evaluating the performance of existing ones requires the selection of critical events, commonly referred to as “design events”. The procedure used to define design events clearly depends on the type of structure. For example, some hydraulic infrastructures, such as sewer pipes, culverts or gullies, usually require the peak flow as the only design parameter. Conversely, reservoirs and dams require a more detailed understanding of the “design hydrograph”.

The design hydrograph for reservoirs and dams can either represent an observed flood event (Dimas et al., 2025) or a synthetic one that synthesises and preserves some physical properties and statistical information about the flow time series (Aureli et al., 2023; Mediero et al., 2010; Michailidi and Bacchi, 2017). However, most basins are ungauged, thus, flow time series are often unavailable, statistically sparse, or limited to annual peak flows, making it challenging to derive past events or construct



30 reliable design hydrographs directly (Evangelista et al., 2023). As a result, it is common to rely on indirect procedures to  
estimate design hydrographs according to rainfall-runoff models. These procedures span a wide spectrum of complexity. At  
one end, rigorous distributed or semi-distributed hydrological models simulate the physical processes governing runoff  
generation and routing in the upstream basin, accounting for spatial variability in precipitation, land cover, soil properties, and  
topography. At the other end, simplified lumped rainfall-runoff models aggregate catchment behaviour into a set of parameters  
35 with clear physical meaning, offering more practical implementations. The choice of modelling strategy is therefore strongly  
conditioned by data availability. Indeed, when detailed hydrometeorological datasets exist, more advanced process-based  
models can be applied; in ungauged or poorly gauged contexts, practitioners are often constrained to lumped rainfall-runoff  
models. Indeed, rainfall time series and Intensity Duration Frequency (IDF) curve parameters are typically more numerous  
and geographically uniform than flow records, and rainfall-runoff models are usually based on a few parameters with a clear  
40 physical meaning (Cristiano et al., 2017).

Among the various indirect methods for estimating design hydrographs for reservoirs and dams, a widely used approach  
involves transforming a design hyetograph, or design storm, with a specified return period into the corresponding design  
hydrograph. This event-based method is broadly adopted for its straightforward implementation (Fischer et al., 2025). One of  
its key advantages is its relatively low computational cost compared to continuous simulation approaches, making it an efficient  
45 tool for reservoir design. Additionally, the method enables rapid comparison of multiple reservoir configurations, and the  
performance of different storage and discharge strategies. However, this procedure presents some concerns. First, it assumes  
that the return period of the resulting hydrograph matches the one of the design hyetograph, which is indeed a strong  
assumption that may not always hold (Aureli et al., 2023; Balistocchi et al., 2013). Moreover, the approach assumes that the  
reservoir storage capacity is empty at the time of the flood event, which may not reflect real-world conditions. Another  
50 limitation is that the method sizes the system based on a single return period, even though a hydrograph is defined by multiple  
factors, such as peak discharge, flood volume and duration, which can have different return periods within the same event,  
adding uncertainty to the design process (Requena et al., 2013).

Another approach to indirectly estimating design hydrographs involves transforming a rainfall time series into a flow time  
series by a continuous simulation using rainfall-runoff models (Pirone et al., 2024). This method provides a more precise  
55 estimation of return periods, as it accounts for real storm temporal sequences and ensures that rainfall distributions are fitted  
based on the complete set of observed events (Balistocchi et al., 2013). Additionally, the rainfall model captures a wide range  
of storm characteristics, including variations in volume, duration, and antecedent dry weather conditions. However, continuous  
simulations require extensive rainfall time series data, often stochastically generated, and are computationally intensive,  
making them less practical when multiple reservoir configurations need to be analysed. As a result, this methodology is  
60 typically applied to specific case studies and is challenging to scale for broader applications (Evangelista et al., 2023).

Given these challenges, the continuous modelling procedure is less used for critical infrastructure such as reservoirs and dams, and using a design hyetograph remains the prevailing solution. However, no universal guidelines suggest which combination of design hyetograph and rainfall-runoff model should be used to estimate the input design hydrograph for reservoirs and dams. Designers navigate conflicting methodologies and guidelines, often without clear evidence supporting the pros and cons of one approach over another. In addition, simulating how the design hydrograph routes through a reservoir is computationally intensive, making exploring all possible input design hydrographs impractical. As a result, the design criteria commonly follow the suggestions and prescriptions outlined by specific local authorities, which widely differ worldwide (Lempérière, 2017).

This study investigates how sensitive reservoir and dam design is to the choice of the input hydrograph by quantifying the differences in reservoir key parameters, such as the maximum outflow discharge, maximum storable volume, and peak reduction effect. At first, this study identifies the most commonly used design hyetographs for reservoir and dam design derived from Intensity Duration Frequency (IDF) curves. These hyetographs include the uniform hyetograph with constant intensity during the duration equal to the basin Lag time (Evangelista et al., 2023; Manfreda et al., 2021; Volpi et al., 2018), the Chicago storm hyetograph (Keifer and Chu, 1957), the uniform hyetograph with constant intensity during the critical duration found according to a variational procedure, usually adopted by the Hydrological Neapolitan School (Pirone et al., 2025; Pianese and Rossi, 1984), and the BLUE hyetograph (Veneziano and Villani, 1999). These hyetographs are transformed into the corresponding hydrographs according to commonly used linear and stationary models: the Linear Reservoir model, the Nash cascade model with 2, 3, and 4 reservoirs, and the Kinematic Wave model. This procedure results in 20 design hydrographs created by combining the four hyetographs with the five rainfall-runoff models. Then, these design hydrographs are routed into reservoirs of different configurations in order to compute the maximum outflow discharge, the maximum storable volume, and the peak reduction effect. On the other hand, this study considers a rainfall time series and transforms it into the corresponding flow time series (according to the five chosen rainfall-runoff models) and routes them into reservoirs of different configurations. This process allows for computing the mean Annual Maxima of the maximum outflow discharge, maximum storable volume, and peak reduction effect to be used as benchmark values. Finally, the result of the reservoir routing are compared in terms of the maximum outflows, stored volume, and peak reduction effect produced by each design hydrograph with those obtained from the continuous flow time series routing.

Since the selection of design hydrographs remains a critical yet often underexamined aspect of reservoir and dam engineering, this study seeks to broaden the understanding of how current hydrograph choice practices may introduce biases or oversimplifications into design processes. By evaluating the performance of existing design hydrographs, this research encourages a more deliberate and evidence-based approach to reservoir and dam design. In addressing the computational demands of detailed reservoir routing, the study also explores pathways toward more efficient modelling without sacrificing critical design reliability.



## 2 Theoretical background

### 2.1 Rainfall-runoff modelling

Under the assumptions of linearity and stationarity in the rainfall-runoff process, the runoff from the basin upstream of the reservoir is obtained through the convolution integral (Eq. 1) by defining the effective inflow discharge  $p(t)$ , hence the fraction of rainfall that reaches the basin as surface runoff, and the Instantaneous Unit Hydrograph (IUH,  $u(t)$ ):

$$Q_t = \int_0^t p(\tau)u(t - \tau)d\tau \quad (1)$$

For the sake of simplicity, the inflow discharge  $p(t)$  can be obtained according to the rational method by subtracting the effective inflow discharge from the hietograph:

$$p(t) = \varphi i(t) A_b \quad (2)$$

where  $\varphi$  is the rational coefficient (representing the fraction of the impervious basin area),  $i(t)$  is the rainfall, and  $A_b$  is the basin area.

### 2.2 Reservoir routing

Once the inflow hydrograph is known ( $Q_{in} = Q_t$ ), it is routed through the reservoir by solving a system of three equations, which comprises 1) the continuity equation, 2) the energy conservation equation in the form of an outlet discharge equation, and 3) a relationship describing the configuration of the reservoir as a function of water depth in it (Eq.s 3):

$$\begin{cases} Q_{in}(t) - Q_{out}(t) = \frac{dW(t)}{dt} \\ Q_{out}(t) = c [h(t)]^n \\ W(t) = \alpha [h(t)]^m \end{cases} \quad (3)$$

where  $Q_{in}(t)$  and  $Q_{out}(t)$  are the inflow and outflow discharges,  $W(t)$  is the water volume in the reservoir, and  $t$  is the time;  $h(t)$  is the water level in the reservoir at time  $t$ ,  $c$  and  $n$  are constant values varying according to outlet type and geometry. For spillways,  $c = \mu_s L \sqrt{2g}$ ,  $n = 1.5$ , and  $h(t)$  is measured from the crest of the spillway ( $h_s$ ) of length  $L$ , and  $\mu_s$  is the discharge coefficient, approximately equal to 0.48. For bottom outlets,  $c = \mu_B \sigma \sqrt{2g}$ ,  $n = 0.5$ , and  $h(t)$  is measured from the centreline of the outlet for submerged ones,  $\mu_B$  is the discharge coefficient, approximately equal to 0.60, and  $\sigma$  is the water section, which for a rectangular section becomes  $B \cdot A$ , with  $B$  the width and  $A$  the height. Finally,  $g$  is the gravitational constant.

The governing storage equations (Eqs. 3) are valid when the water surface is horizontal, that is, the outflow is unaffected by tailwater. When combined, they give a nonlinear first-order ordinary differential equation whose solution requires numerical methods such as the method of finite differences.



### 3 Methodology

By assuming linearity and stationarity in the rainfall-runoff process, we consider a case study consisting of a basin upstream of a reservoir and a rainfall time series. In this setup, we first convert the rainfall time series into the corresponding flow time series. To this aim, five rainfall-runoff models are used: the Linear Reservoir model, the Nash cascade model with 2, 3, and 4 reservoirs, and the Kinematic Wave model. Next, we route the flow time series into different reservoir configurations to evaluate the reservoirs effect and compute the outflow time series. From the outflow time series, we extract key parameters such as the mean Annual Maxima of the maximum outflow discharge, maximum storable volume, and peak reduction effect, which are used as benchmark parameters. Then, starting from the rainfall time series, we estimate the IDF curves parameters and the selected design hyetographs: the Uniform hyetograph, the Chicago Storm hyetograph, the Uniform hyetograph with a duration found according to the variational procedure (hereafter referred to as Variational hyetograph), and the BLUE hyetograph. This process results in 20 design hydrographs created by combining the four hyetographs with the five rainfall-runoff models. Finally, these hydrographs are routed into the reservoir to compute maximum outflow discharge, maximum storable volume, and peak reduction effect, and compare them with the benchmark cases, obtained from the continuous rainfall-runoff routing of the time series.

#### 3.1 Rainfall-runoff modelling

The rainfall-runoff modelling requires the definition of the basin upstream of the reservoir configuration, the rainfall pattern (rainfall time series or design hyetograph) and the Instantaneous Unit Hydrograph (Eqs. 1-2). At first, the rainfall time series is convoluted according to Eq. 1 to obtain the corresponding flow time series. Then, design hyetographs (Fig. 2) are constructed after estimation of the IDF curve parameters from the same rainfall time series.

##### 3.1.1 IDF curves

A tri-parametric expression was chosen to estimate the parameters of the IDF curves (Eq. 4):

$$i_d = \frac{I_0}{\left(1 + \frac{d}{d_c}\right)^\beta} \quad (4)$$

where  $d$  is the rainfall duration,  $i_d$  is the mean of the annual maxima of the rainfall intensity averaged over the rainfall duration  $d$ , and  $I_0$ ,  $d_c$  and  $\beta$  are parameters obtained from the rainfall time series by interpolating observed values of couples  $(d, i_d)$ . It is worth noting that the IDF curve selected in this study is independent of the return period. To account for it, users must choose a probabilistic model to determine the growth factor  $K_T$  with return period  $T$  of the variable  $i_d$ , which adjusts Eq. 4 accordingly.

$$i_{d,T} = i_d \cdot K_T \quad (5)$$

The simulations here assume  $K_T=1$ , representing the base condition without return period adjustments.



### 3.1.2 Design hyetographs

Once the IDF curves parameters have been estimated, it is possible to construct the selected design hyetographs: the Uniform hyetograph, the Chicago Storm, the Variational hyetograph and the BLUE hyetograph.

The Uniform hyetograph (Eq. 6) is a rectangular rainfall event with a duration equal to the Lag time of the basin and a constant intensity extracted from the IDF curve:

150

$$i_{L_t} = \begin{cases} \frac{I_0}{\left(1 + \frac{L_t}{d_c}\right)^\beta} & \text{if } t \leq L_t \\ 0 & \text{otherwise} \end{cases} \quad (6)$$

The Chicago hyetograph (Keifer and Chu, 1957; Eq. 7) is designed to align rainfall intensity with the IDF curve for all durations. It enables a single synthetic storm to embed a given rainfall return level for all durations of interest based on the IDF curve (Peleg et al., 2024). Alfieri et al. (2008) provided the Chicago hyetograph formulation valid for a three-parametric (x, y and z) expression of the IDF curve:

155

$$i(t) = \begin{cases} x \frac{y + (1-z) \frac{t_r - t}{r_c}}{\left(y + \frac{t_r - t}{r_c}\right)^{z+1}} & \text{if } t \leq t_r \\ x \frac{y + (1-z) \frac{t - t_r}{1 - r_c}}{\left(y + \frac{t - t_r}{1 - r_c}\right)^{z+1}} & \text{if } t > t_r \end{cases} \quad (7)$$

where  $x = I_0 d_c^\beta$ ,  $y = d_c$ ,  $z = \beta$ ,  $r_c = t_r / t_c$  thus, the ratio between the peak position  $t_r$  and the concentration time of the basin  $t_c$ . In this study, the peak position of the Chicago hyetograph is always set to the midpoint, i.e.,  $r_c = 0.5$ . Moreover, we assumed that the time of concentration of the basin is twice the Lag time of the basin, which equals to state that the basin has a rectangular shape (Rossi and Villani, 1995).

160

The Variational hyetograph is a rectangular rainfall event with constant intensity during the critical duration  $d$  extracted from the IDF curve. The critical duration is a duration that maximises a variable of interest and can be found according to a variational procedure, hence the name “Variational hyetograph”. For example, the variable of interest could be the outflow from the reservoir or the maximum storable volume. The variational procedure can be summarised as follows: i) a trial rainfall duration  $d$  is chosen; ii) the corresponding intensity  $i_d$  is evaluated from the IDF curve (Eq. 4); iii) a rectangular rainfall event with constant intensity during the duration  $d$  extracted from the IDF curve is considered (Eq. 8); iv) Eq. 1 is solved, hence, the inflow hydrograph associated with the chosen duration  $d$  is evaluated; v) the inflow hydrograph is propagated through the reservoir to obtain the outflow hydrograph and the maximum outflow discharge (or another variable of interest, such as the maximum storable volume); vi) a new rainfall durations  $d$  is set, and the procedure is repeated for each duration from point ii) to point v) until the duration  $d^*$  that provides the maximum outflow discharge from the reservoir is identified.

170



$$i_d(t) = \begin{cases} \frac{I_0}{\left(1+\frac{d}{d_c}\right)^\beta} & \text{if } t \leq d \\ 0 & \text{otherwise} \end{cases} \quad (8)$$

Finally, the BLUE hyetograph (Eq. 9) is a rainfall event associated with any given flood discharge  $Q$ , using Best Linear Unbiased Estimation (BLUE) theory. It depends explicitly on the correlation characteristics of the rainfall process and the IUH of the basin. When the correlation time of the rainfall process is short relative to the dispersion of the IUH, the shape of the BLUE hyetograph is the mirror image of the IUH itself (Veneziano and Villani, 1999):

$$i_{BLUE}(\tau) = Q \frac{u(\tau)}{\int_0^\infty u^2(\tau) d\tau} \quad (9)$$

where  $i_{BLUE}$  is the rainfall intensity in  $\tau$  units of time before the maximum discharge  $Q$  is reached. The maximum discharge  $Q$  is an unknown quantity, hence, further assumptions must be made. For example, Alfieri et al. (2008) assumed that the total amount of rainfall carried by the BLUE hyetograph was congruent with the IDF curves, thus they considered that the ratio  $Q / \int_0^\infty u^2(\tau) d\tau$  was equal to the rain depth computed from the IDF curve at the time of concentration of the basin. In their case, however, the BLUE hyetograph produced rainfall intensities that exceeded the IDF curve. Indeed, the distribution of the rainfall intensities within the hyetograph was constrained only by the shape of the IUH of the basin. Therefore, this study does not adopt the previously described procedure, but considers that the maximum discharge  $Q$  of Eq. 9 equals the mean Annual Maxima of the instantaneous  $Q_{in}$ . This value is computed after transforming the rainfall time series into the corresponding flow time series. Therefore, this study considers that the BLUE hyetograph does not depend on the IDF parameters, but rather on the mean Annual Maxima of the instantaneous  $Q_{in}$ .

### 3.1.3 IUH

This study considers five linear and stationary runoff models (Table 1): the Linear Reservoir (LR) model, the Nash model with 2, 3, and 4 reservoirs (N2, N3, and N4), and the Kinematic Wave model with a rectangular shape of the basin (KW).

**Table 1: Instantaneous Unit Hydrograph (IUH) and United Hydrograph  $S(t)$  of the selected rainfall-runoff models and their parameters.**

Rainfall-runoff model	IUH	$S(t)$	Parameters
Linear Reservoir (LR)	$u(z) = \frac{1}{L_t} e^{-\frac{z}{L_t}}$	$S(z) = 1 - e^{-\frac{z}{L_t}}$	$L_t$
Nash with 2 reservoirs (N2)	$u(z) = \frac{z}{L_{t,N2}^2} e^{-\frac{z}{L_{t,N2}}}$	$S(z) = 1 - \frac{e^{-\frac{z}{L_{t,N2}}}(L_{t,N2} + z)}{L_{t,N2}}$	$L_{t,N2} = \frac{L_t}{2}$
Nash with 3 reservoirs (N3)	$u(z) = \frac{z^2}{2L_{t,N3}^3} e^{-\frac{z}{L_{t,N3}}}$	$S(z) = 1 - \frac{e^{-\frac{z}{L_{t,N3}}}(2L_{t,N3}^2 + 2L_{t,N3}z + z^2)}{2L_{t,N3}^2}$	$L_{t,N3} = \frac{L_t}{3}$
Nash with 4 reservoirs (N4)	$u(z) = \frac{z^3}{6L_{t,N4}^4} e^{-\frac{z}{L_{t,N4}}}$	$S(z) = 1 - \frac{e^{-\frac{z}{L_{t,N4}}}(6L_{t,N4}^3 + 6L_{t,N4}^2z + 3L_{t,N4}z^2 + z^3)}{6L_{t,N4}^3}$	$L_{t,N4} = \frac{L_t}{4}$



Kinematic Wave (KW)	$u(z) = \begin{cases} \frac{1}{t_c} & \text{if } z \leq t_c \\ 0 & \text{if } z > t_c \end{cases}$	$S(z) = \begin{cases} \frac{z}{t_c} & \text{if } z \leq t_c \\ 1 & \text{if } z > t_c \end{cases}$	$t_c = 2L_t$
------------------------	--	--	--------------

The parameters of the runoff models are chosen coherently to ensure a fair and meaningful comparison (Fig. 1). Thus, the basin Area, its imperviousness, and the Lag time are the same. In particular, the Lag time of the Nash model with two reservoirs ( $L_{t,N2}$ ) is set at half the time of the Lag time of the Linear Reservoir model, and the time of concentration,  $t_c$  of the Kinematic Wave model with rectangular shape is set twice the Lag time (Table 1).

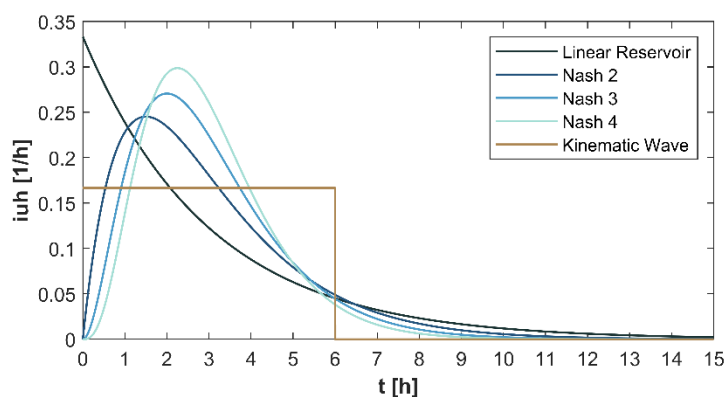


**Figure 1: Instantaneous Unit Hydrograph (IUH) of the five rainfall-runoff models: the Linear Reservoir model, the Nash model with 2, 3, and 4 reservoirs, and the kinematic wave model. The Lag time used to create the graph is 3 hours. Colours follow recommendations of scientifically derived colour maps (Crameri et al., 2020).**

### 3.2 Reservoir routing

For each IUH, the rainfall-runoff modelling (section 3.1) provides the input for the reservoir routing, thus a synthetic flow time series and 4 design hydrographs. These inputs are routed into reservoirs of different configurations (Fig. 2) and the maximum outflow discharge (peak outflow)  $Q^*_{out}$ , the maximum stored volume, and the peak reduction effect are evaluated.

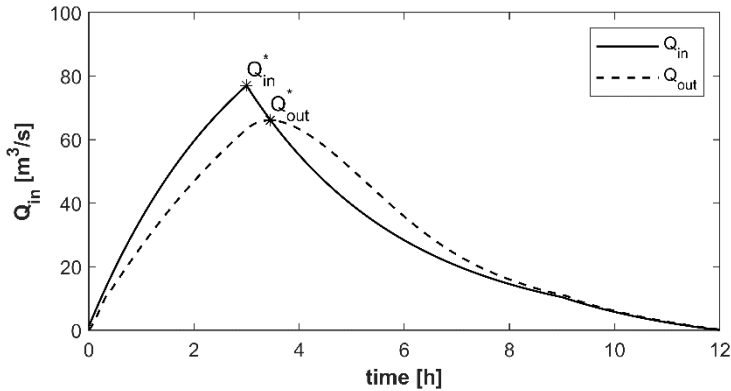


**Figure 2: Example of a reservoir routing obtained via numerical simulation. The input hydrograph represented in this figure is obtained considering the Linear Reservoir as rainfall-runoff model and the Uniform hyetograph as design hyetograph.**

In particular, the peak reduction effect is computed as the ratio between the peak outflow,  $Q_{out}^*$ , and peak inflow,  $Q_{in}^*$  (Eq. 9).

$$\eta = \frac{Q_{out}^*}{Q_{in}^*} \quad (10)$$

For the procedure that considers the continuous rainfall-runoff modelling from the rainfall time series, these parameters (the maximum outflow discharge, the maximum stored volume, and the peak reduction effect) can be evaluated for each year as mean Annual Maxima, and are referred hereafter to as “mean Annual Maxima”.

## 4 Case studies

We considered two types of case studies to evaluate the effect of the input design hydrograph on reservoir configuration: a series of synthetic test cases consisting of i) a rainfall time series, a basin upstream of the reservoir, and 48 reservoir configurations, and ii) a real-world case dam with the corresponding basin upstream the reservoir and rainfall times series.

### 4.1 Synthetic test cases

#### 4.1.1 Basin parameters and rainfall Time Series

The synthetic test cases were based on a reference basin characterised by the parameters listed in Table 2 (Pirone et al., 2025). The rainfall time series used in the analysis was obtained from the Multihazard Functional Center of the Civil Protection Department of the Campania Region (Italy). Specifically, the data were recorded at the “Grazzanise” monitoring station, a pluviographic station operating since 1999 with a temporal resolution of 10 minutes (Morbidelli et al., 2025). From this rainfall time series, the parameters of the Intensity-Duration-Frequency (IDF) curve (Table 2) were derived using Eq. 4, based on the mean Annual Maxima for various durations (Fig. 3).



225 **Table 2: Basin parameters.**

Element	Parameter	Value
Basin	Area $A_b$ [km <sup>2</sup> ]	100
	Lag time $L_t$ [h]	3
	rational coefficient $\varphi$ [-]	0.30
IDF curves	$I_0$ [mm/h]	119.572
	$d_c$ [h]	0.229
	$\beta$	0.798

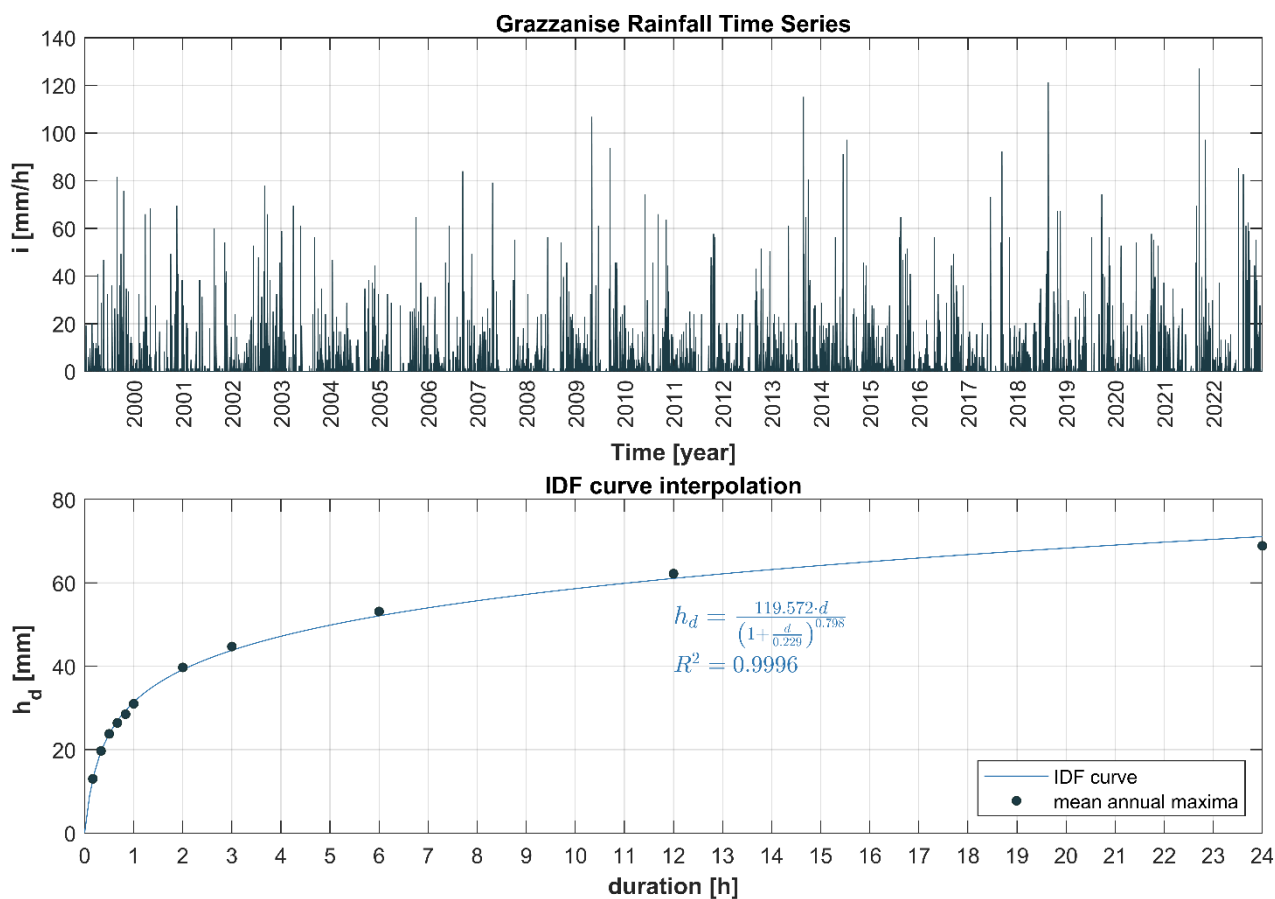


**Figure 3. Rainfall time series recorded at the Grazzanise station (top), and Intensity-Duration-Frequency (IDF) curves (bottom), derived by interpolating the mean Annual Maxima from the rainfall time series.  $R^2$  represents the correlation coefficient.**

#### 4.1.2 Design hydrographs

230 According to the parameters of Table 2 and Eqs. 6 to 9, the design hydrographs for the five runoff models (Table 1) were evaluated (Fig. 4).

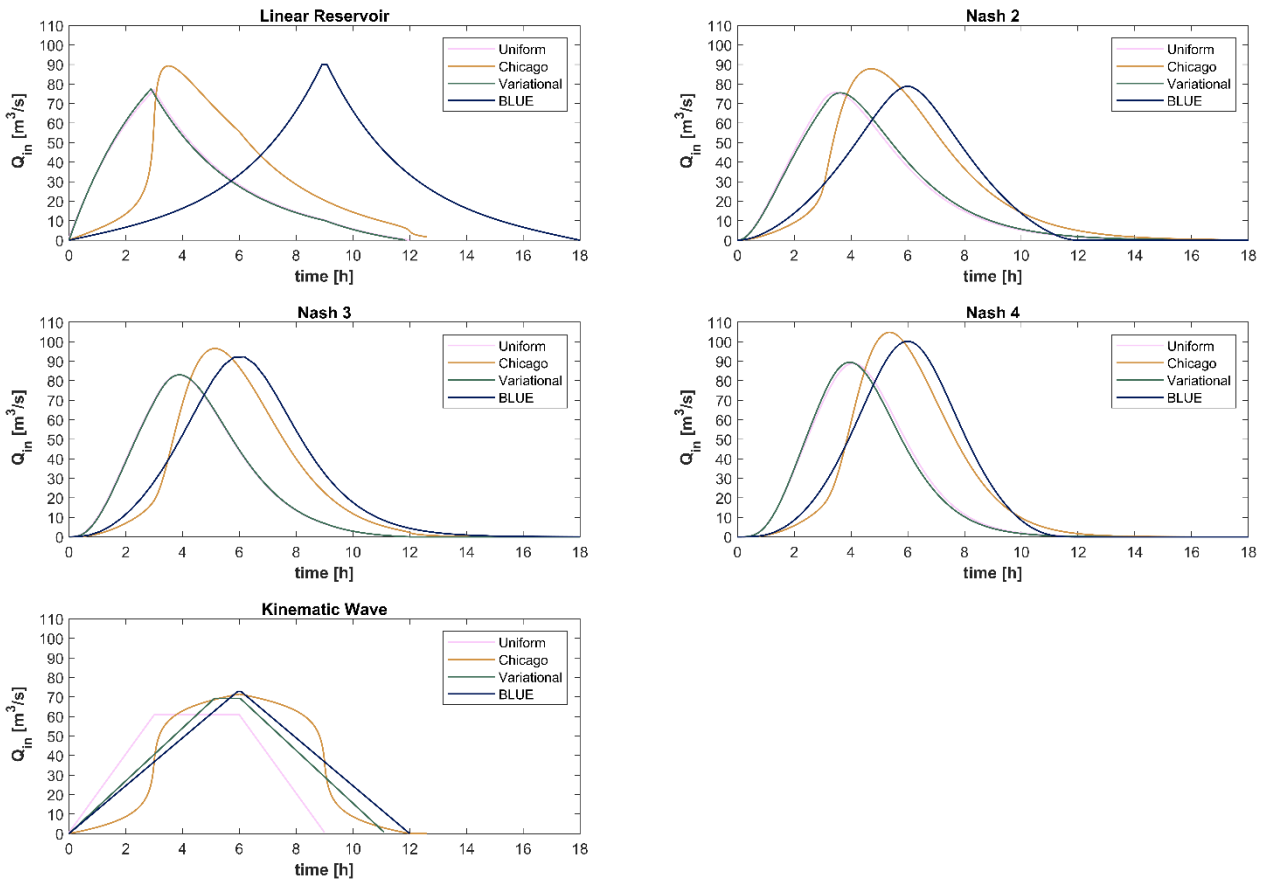


**Figure 4: Design hyetographs (Uniform, Chicago, Variational, and BLUE) grouped according to the IUH a) Linear Reservoir, b) Nash model with 2 reservoirs, c) Nash model with 3 reservoirs, d) Nash model with 4 reservoirs, and e) Kinematic Wave model.**

235 **4.1.3 Reservoir configurations**

Finally, 48 reservoir configurations (Table 3) were considered by combining three outlet structure configurations (parameters  $n$  and  $c$  of Eqs. 3) with 16 reservoir geometries configurations (parameters  $\alpha$  and  $m$  of Eqs. 3). The values of  $c$  correspond to rectangular shape bottom outlets with a cross-section ( $B \times A$ ) = (2.0 m  $\times$  2.0 m), (2.5 m  $\times$  2.5m), and (3.0 m  $\times$  3.0 m). These reservoir combinations were also derived from the configurations used by Pirone et al. (2025), which were developed based on the reference basin.

240

**Table 3. Reservoir parameters describing stage-storage and stage-discharge curves (Eqs. 3).**

Element	Parameter	Value
Reservoir	$\alpha$ [m <sup>3</sup> ]	3000; 6000
	$m$ [-]	1.0; 1.5; 2.0; 2.5; 3.0; 3.5; 4.0; 4.5



n [-]	0.5
c [m <sup>3-n</sup> /s]	10.63; 16.61; 23.91

#### 4.2 Real-world test case: San Giovanni Dam

The impact of different input hydrographs on reservoir design is also assessed using a real-world test case, the San Giovanni Dam. This evaluation serves both sizing and verification purposes: verification, by comparing the maximum outflow discharge and thus the peak reduction effect (Eq. 10), obtained with different design hydrographs and the rainfall Time Series and sizing, by analysing the maximum storable volumes.

The San Giovanni Dam is an in-line dam on the Palistro River in Southern Italy. The dam serves a basin upstream of 0.170 km<sup>2</sup> (Fig. 5), characterised by a Lag time of 0.489 h and a runoff coefficient of 0.9 (Pirone et al., 2025). The nearest rain gauge is “Vallo della Lucania”, about 4.6 km far and located at 377 m a.s.l., which is comparable to the basin mean elevation (338.2 m a.s.l.). The Multihazard Functional Center of the Civil Protection Department of Campania Region provided a 17 years long rainfall Time Series (from 2008), from which IDF curve parameters (Table 4) were evaluated according to Eq. 4. The Linear Reservoir model was chosen to model the runoff of the basin upstream of the reservoir.

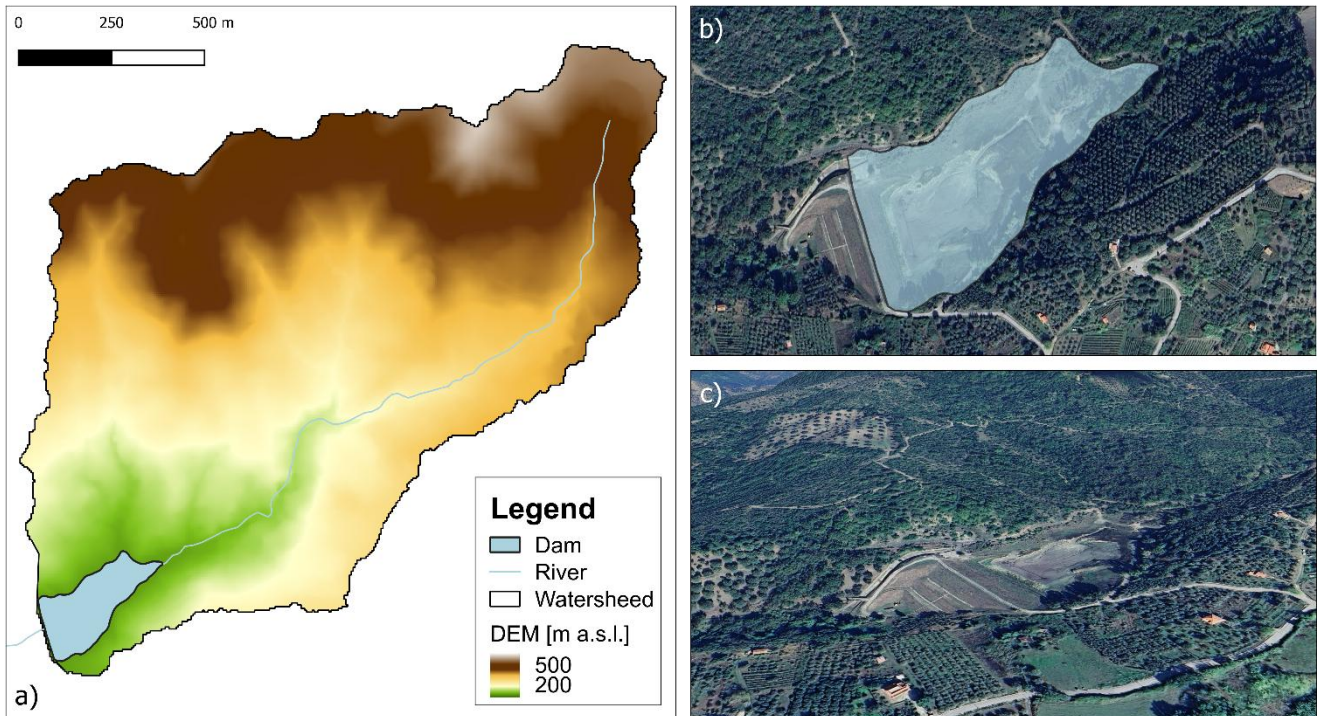


Figure 5: a) San Giovanni Dam with the corresponding basin upstream and the main stream segments of the River; b) 2D areal view of the San Giovanni Dam; c) 3D view of the San Giovanni Dam (from © Google Earth) .



The dam is characterised by a height of 18 m, a surface area of about 40'000 m<sup>2</sup> and a storage volume of about 300'000 m<sup>3</sup> (Evangelista et al., 2024). Its primary purpose is for agricultural use; thus, the flood attenuation is operated by a spillway at 15.3 m. Pirone et al. (2025) provided the values (C, n, α and m of Eqs. 2) valid for the spillway, thus from water level above 15.3 m to 18 m. Therefore, the parameters of Table 4 have been considered for the reservoir geometry and bottom outlet structures, as well as the stage-outflow and stage-discharge curves.

**Table 4: San Giovanni Dam parameters.**

Element	Parameter	Value
Basin upstream	Area A <sub>b</sub> [km <sup>2</sup> ]	1.746
	Lag time L <sub>t</sub> [h]	0.489
	rational coefficient φ [-]	0.900
IDF curves	I <sub>0</sub> [mm/h]	183.830
	dc [h]	0.067
	β	0.703
Dam configuration	c	0.070
	n	0.455
	α	1567.750
	m	1.994

## 5 Results and Discussions

Given a rainfall-runoff model, the maximum outflow discharge, the maximum storable volume, and the peak reduction effect of the reservoirs are compared, considering the values obtained from the flow time series as the reference values (benchmark).

The performance criteria used is the mean percentage error, Eq. 11:

$$err_{\%} = \frac{1}{n} \sum_{i=1}^n \frac{\hat{x}_i - x_i}{x_i} \quad (11)$$

where  $\hat{x}_i$  is the reference value (maximum outflow discharge, maximum storable volume, and peak reduction effect),  $x_i$  is the estimated value (according to the design hyetograph), and  $i$  is the  $i$ -th reservoir configuration.

### 5.1 Synthetic test cases

#### 5.1.1 Maximum outflow discharge

The mean percentage errors (Eq. 10) of the maximum outflow discharge between the mean Annual Maxima and the four design hyetographs for the five rainfall-runoff models are presented in Table 5.

**Table 5: Mean percentage errors of the outflow discharge between the reference value (Mean Annual Maxima) and the design hyetographs (Uniform, Chicago, Variational and BLUE) for the five rainfall-runoff models.**

	Uniform	Chicago	Variational	BLUE
--	---------	---------	-------------	------



---

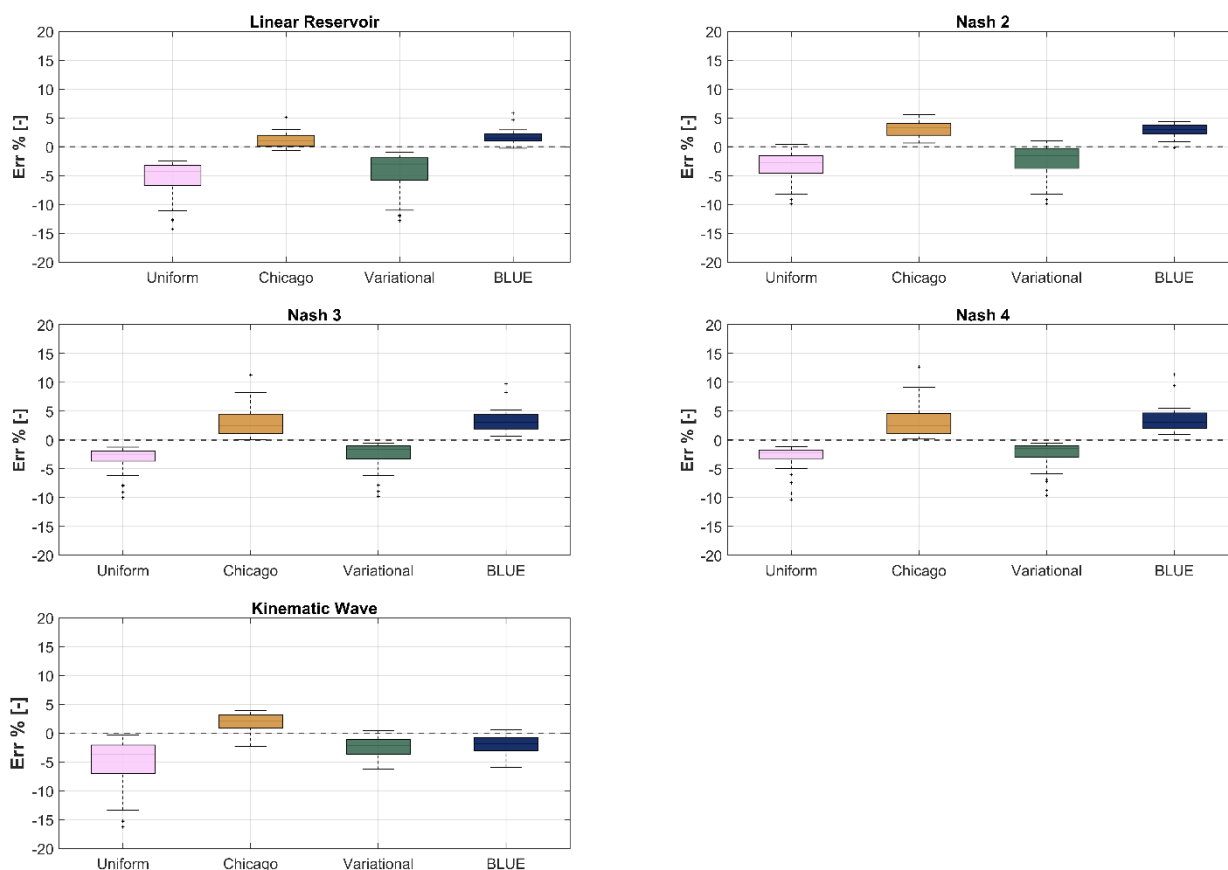
Linear Reservoir	-5.2%	1.1%	-4.2%	1.7%
Nash with 2 reservoirs	-3.3%	3.0%	-2.4%	3.0%
Nash with 3 reservoirs	-3.2%	3.0%	-2.5%	3.3%
Nash with 4 reservoirs	-3.0%	3.1%	-2.4%	3.5%
Kinematic Wave	-5.1%	1.8%	-2.3%	-1.9%

---

275

The Uniform hyetograph (first column of Table 5) produces negative mean percentage errors, indicating an overall underestimation of the maximum outflow discharge compared to those obtained from the rainfall time series (mean Annual Maxima). The Chicago hyetograph, in contrast, exhibits lower positive errors, indicating a tendency to slightly overestimate the maximum outflow discharge, with errors ranging from 1.1% to 3.1%. The Variational hyetograph shows relatively small negative errors, ranging from -4.2% to -2.3%. Finally, the BLUE hyetograph (last column of Table 5) is the only one that switches between positive and negative errors: most models exhibit slight overestimation, ranging from 1.7% to 3.5%, while the KW model shows a slight underestimation (-1.9%). These trends are also shown in Fig. 6, together with the range of variability of the errors.

280



285

**Figure 6: Percentage error (Err%) distributions between the maximum outflow from the reservoirs obtained from the continuous rainfall-runoff time series and those obtained from the four design hyetographs—Uniform, Chicago, Variational, and BLUE—for the five rainfall-runoff models: a) Linear Reservoir, b) Nash model with 2 reservoirs, c) Nash model with 3 reservoirs, d) Nash model with 4 reservoirs, and e) Kinematic Wave model.**

290 The results demonstrate that all the selected design hyetographs can closely replicate the maximum outflow discharges obtained from continuous flow time series routing. While the low percentage of errors achieved confirms the general applicability of all of the selected hyetographs, the variability in performance among them reveals critical considerations for reservoir design.

295 Firstly, a key insight emerging from these results is that the assumption underpinning the Uniform hyetograph that the basin Lag time corresponds to the critical storm duration can be an oversimplification. While commonly adopted due to its analytical solution in reservoir routing with spillway outlets (Manfreda et al., 2021; Volpi et al., 2018), the assumption of the Uniform hyetograph can lead to the underestimation of the maximum outflow discharge. This insight is further confirmed by the Variational hyetograph results, which achieved lower errors by identifying rainfall durations that differ from the basin Lag time. Therefore, the widespread assumption that the Lag time inherently represents the critical duration for reservoir and dam



300 design may not always hold true, and design methods that treat it as such should be carefully revised. Some studies also  
consider a Uniform hyetograph with a duration equal to the time of concentration of the basin (Evangelista et al., 2023).  
However, this approach requires additional assumptions regarding the relationship between the basin Lag time and its time of  
concentration. For instance, some authors assume a ratio of two (Rossi and Villani, 1995), while others use a ratio of 1.5  
305 (Sultan et al., 2022), depending on the basin morphology. In this context, the Variational approach employed to identify the  
critical rainfall duration of the Variational hyetograph helps reduce the subjectivity associated with selecting the hyetograph  
duration, offering a more objective and physically consistent framework. However, despite its improved accuracy, the  
procedure to identify the Variational hyetograph is computationally intensive; thus, its practicality should be significantly  
improved, for example, by coupling it with optimisation algorithms. Notably, Pirone et al. (2025) proposed a Semi-Analytical  
Approach to identify the critical hydrograph and, thus, the hydrograph providing the maximum outlet discharge from the  
310 reservoir. Their approach makes the Variational hyetograph more feasible, especially in scenarios involving multiple reservoir  
configurations for sizing and comparative analyses.

Another noteworthy finding that emerged from these results is the strong performance of the BLUE hyetograph in estimating  
the maximum outflow discharge, which produced highly accurate results using only the peak values from the mean annual  
maxima inflow series. This result demonstrates that the BLUE hyetograph is particularly appealing in contexts where flow  
315 time series are available or even when only annual peak inflows are available, as it effectively bypasses the need for the IDF  
curve parameters or the complete time series. However, the BLUE hyetograph applicability is limited in data-scarce or  
ungauged regions, where rainfall or flow time series may not be available, reducing its utility in such contexts.

### 5.1.2 Maximum storable volume

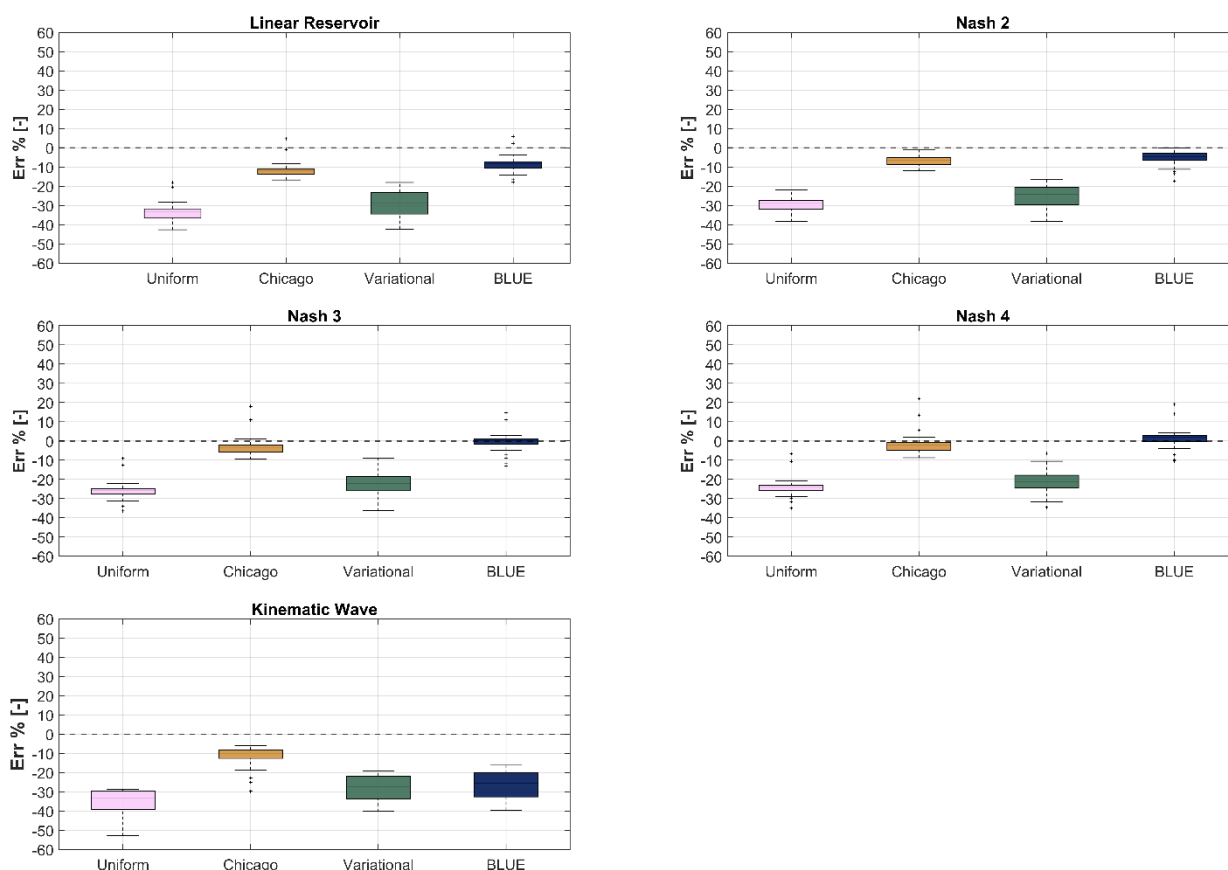
The mean percentage errors (Eq. 10) of the maximum storable volumes between the mean Annual Maxima and the four design  
320 hyetographs for the five rainfall-runoff models are presented in Table 6.

**Table 6: Mean percentage errors of the maximum storable volume discharge between the reference value (Mean Annual Maxima) and the design hyetographs (Uniform, Chicago, Variational and BLUE) for the 5 rainfall-runoff models.**

	Uniform	Chicago	Variational	BLUE
Linear Reservoir	-33.4%	-11.8%	-28.9%	-8.5%
Nash with 2 reservoirs	-29.3%	-6.8%	-25.1%	-5.3%
Nash with 3 reservoirs	-25.9%	-3.5%	-22.4%	-0.5%
Nash with 4 reservoirs	-24.2%	-2.1%	-21.3%	1.3%
Kinematic Wave	-35.2%	-11.4%	-28.0%	-26.6%



325 The Uniform and Variational hyetograph tend to underestimate maximum storable volumes, with Variational exhibiting smaller errors overall. The Chicago hyetograph also underestimates but has much smaller errors, making it more reliable than Uniform for estimating volumes. Meanwhile, the BLUE hyetograph produces the lowest overestimation in most models and a notable underestimation in the Kinematic Wave model. These trends are also shown in Fig. 7, as long as the range of variability of the errors.



330 **Figure 7: Percentage error (Err%) distributions between the maximum outflow from the reservoirs obtained from the continuous rainfall-runoff time series and those obtained from the four design hyetographs—Uniform, Chicago, Variational, and BLUE— for the five rainfall-runoff models: a) Linear Reservoir, b) Nash model with 2 reservoirs, c) Nash model with 3 reservoirs, d) Nash model with 4 reservoirs, and e) Kinematic Wave model.**

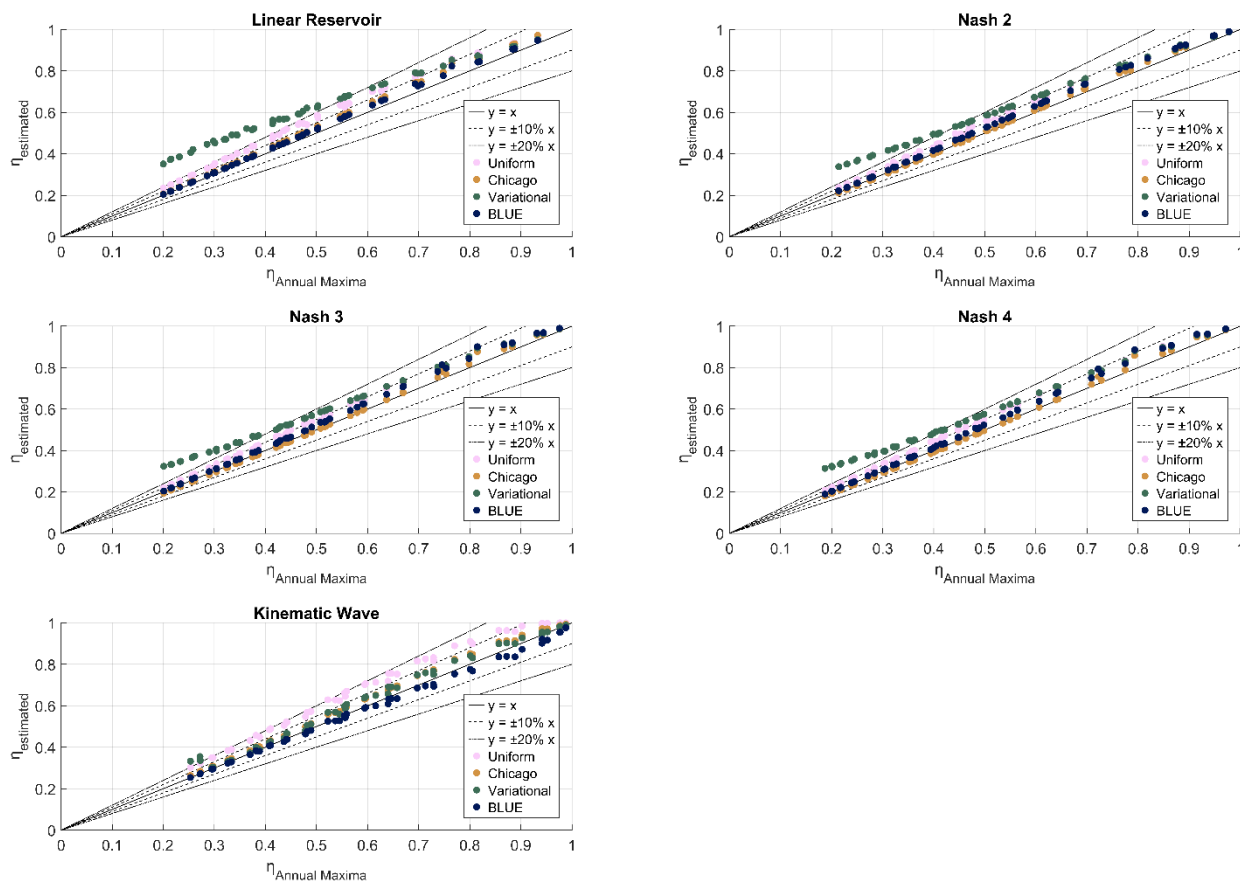
335 Results show that all design hyetographs led to a systematic underestimation of the maximum storable volumes compared to those estimated from continuous time series simulations. These results reveal a significant limitation of event-based design hyetographs in replicating the time series processes. A key factor contributing to these discrepancies is likely the assumption that the full storage volume is available at the beginning of the event. In contrast, continuous time-series routing accounts for the cumulative effects of antecedent conditions, which constrain available storage more realistically. This divergence in initial



340 conditions could be particularly critical in systems where the catchment response time is shorter than the reservoir time to  
release flood volume, as highlighted by previous studies (Aureli et al., 2023; Balistrocchi et al., 2013). Indeed, when inflows  
from rainfall events arrive quickly, but the reservoir requires a longer time to release stored flood volume, successive storm  
events may occur before the reservoir has fully emptied, resulting in residual storage from previous events still occupying part  
of the reservoir volume. Consequently, this mismatch between design hyetograph and flow time series can significantly  
underestimate the volume required to safely store flood, leading to potential design failures. Therefore, a key insight from  
345 these findings is that design hyetographs fail to reproduce the mean annual maxima of stored volume, suggesting that future  
developments should focus on incorporating variable initial storage conditions into event-based modelling frameworks. One  
possible way to further investigate these dynamics is to analyse the autocorrelation function of the time series of inflows and  
reservoir levels. The autocorrelation function can reveal whether past events significantly influence current storage availability,  
suggesting an influence of antecedent conditions, thus supporting the need for continuous routing approaches over event-based  
350 methods. Moreover, further investigation should be conducted to verify the assumption underlying the event-based design  
approach, which posits that the characteristics of an event share the same return period (Requena et al., 2013). Such an  
investigation could help clarify if potential underestimations in maximum storable volume estimates arise from this  
simplification.

### 5.1.3 Peak reduction effect

355 The comparison of the peak reduction effect ( $\eta$ ) obtained from continuous simulations and four design hyetographs reveals  
significant over- and under-estimation trends (Fig. 8). An overestimation of  $\eta$  indicates that the reservoir reduces the inflow  
less than expected, while an underestimation suggests a greater reduction than expected. The Uniform hyetograph consistently  
overestimated  $\eta$  by up to 20% across most runoff models. Similarly, the Chicago hyetograph exhibited an overestimation trend,  
though with smaller deviations, never exceeding 10%. In contrast, the Variational hyetograph resulted in the greatest  
360 overestimation, particularly for the LR model, where deviations exceeded +20% and for lower  $\eta$  values. The magnitude of  
these errors decreased across other rainfall-runoff models, with the KW model exhibiting the most constrained deviations,  
remaining within  $\pm 10\%$ . Finally, the BLUE hyetograph produced estimates closely aligned with those from continuous  
simulations, as reflected in their clustering along the  $y=x$  line, suggesting that the BLUE method is the most robust across  
different models, reinforcing its reliability for peak reduction estimation.



365

**Figure 8: Comparison between the peak reduction effect of the reservoirs obtained from the continuous rainfall-runoff time series and those obtained from the four design hyetographs—Uniform, Chicago, Variational, and BLUE—for the five rainfall-runoff models.**

370

The observed differences in peak reduction estimate highlight that it is highly sensitive to the choice of input hyetograph. From these cases emerged an overestimation associated with the Uniform and Chicago hyetographs, suggesting that these methods may lead to an inflated perception of the reservoir attenuation capacity. The even more significant overestimation observed with the Variational hyetograph indicates that its objective to find the critical duration may lead to unreliable peak reduction estimates. An overestimation of the peak reduction effect implies that the reservoir was expected to attenuate less than it actually does. In a comparative ranking of configurations, an overestimation would artificially lower the perceived performance of the reservoir. Consequently, such a configuration might be ranked lower than it should be, potentially leading to the selection of underperforming designs. Conversely, the BLUE hyetograph demonstrated strong agreement with continuous simulations across different runoff models, reinforcing its robustness as a reliable method for peak reduction estimation. These findings suggest that the BLUE method may be preferable for hydrological design applications where accurate representation of reservoir effects is critical. Therefore, when estimating the peak reduction effect, selecting a suitable

375



380 design hyetograph is critical not only to ensure reliable performance estimates that accurately capture reservoir attenuation behaviour but also to inform sound design decisions. Moreover, accurately assessing peak discharge reduction is essential for flood frequency analysis, as it directly influences the estimation of downstream flood magnitudes and frequencies (Merz et al., 2022). Misrepresenting the attenuation effect can lead to either over- or underestimation of flood risks, compromising the effectiveness of flood management strategies and infrastructure design.

## 385 5.2 Real-world test case: San Giovanni Dam

The maximum outflow discharges, maximum storable volumes and peak reduction effect obtained from the continuous rainfall time series routing (mean Annual Maxima) and the four design hyetographs are presented in Table 7.

**Table 7: Maximum outflow discharge ( $Q_{out}$ ), maximum storable volume ( $W_{max}$ ), and peak reduction effect ( $\eta$ ) obtained from the continuous rainfall time series routing (mean Annual Maxima) and from the four design hyetographs (Uniform, Chicago, Variational, and BLUE). Percentage errors are in square brackets.**

390

	mean Annual Maxima	Uniform	Chicago	Variational	BLUE
$Q_{out}$ [ $m^3/s$ ]	11.53	8.75 [-24.1%]	10.20 [-11.5%]	9.18 [-20.3%]	11.46 [-0.5%]
$W_{max}$ [ $m^3$ ]	8 825	6 273 [-28.9%]	7 561 [-14.3%]	6 654 [-24.6%]	8 701 [-1.4%]
$\eta$ [-]	0.74	0.76 [2.2%]	0.78 [5.9%]	0.85 [14.3%]	0.74 [0.5%]

395

Results indicate that the BLUE hyetograph provides the closest match to the Mean Annual Maxima across all parameters, with minimal errors in peak outflow discharge ( $Q_{out} = -0.55\%$ ) and maximum storable volume ( $W_{max} = -1.41\%$ ), while maintaining the same peak reduction effect ( $\eta = 0.74$ ). The Chicago hyetograph moderately underestimates  $Q_{out}$  (-11.47%) and  $W_{max}$  (-14.32%), whereas the Uniform and Variational hyetographs exhibit the most significant discrepancies, underestimating  $Q_{out}$  by -24.13% and -20.35% and  $W_{max}$  by -28.91% and -24.60%, respectively. Notably, the Variational hyetograph achieves the highest peak reduction ( $\eta = 0.85$ ), suggesting an overestimation of the peak reduction effect, thus, a lower capacity for flow attenuation.

400

The findings from the San Giovanni Dam case study further emphasise the critical role of hyetograph selection in reservoir design, corroborating the insights obtained from the synthetic case studies. In this real-world application, the assumption underlying the Uniform hyetograph that the basin lag time coincides with the critical storm duration was again shown to be invalid. Indeed, the Variational hyetograph performed better in both maximum outflow discharge and maximum storable volume. Among all the selected hyetographs, the BLUE hyetograph was found to be the most reliable option, closely matching the mean Annual Maxima with minimal errors across all the reservoir parameters, making it a preferable choice for reservoir design. The substantial variations observed across key design metrics highlight that a subjective or arbitrary choice of input

405



hyetograph can significantly affect project outcomes. Therefore, the conscious and consistent selection of design hyetograph is essential to ensure consistent and effective reservoir design.

## 6 Conclusions

410 This study investigated how the choice of input hyetograph influences reservoir key parameters, including maximum outflow discharge, maximum storable volume and peak reduction effect. Several important findings emerged by comparing the results of continuous time series routing and commonly used design hyetographs (Uniform, Chicago, Variational, and BLUE).

415 Firstly, all selected design hyetographs closely replicated the maximum outflow discharges obtained from continuous simulations, confirming their general applicability. A critical insight from maximum outflow discharge estimates is that the widespread assumption that basin Lag time represents the critical rainfall duration for reservoir design does not always hold. Notably, the Uniform hyetograph underestimated reservoir key parameters compared to the Variational hyetograph, highlighting the need to find a duration that differs from the basin Lag time and revise design approaches that rely on this assumption rigidly. From a practical standpoint in estimating maximum outflow discharge, this study concludes that the Chicago hyetograph offers computational efficiency for single-reservoir analyses by requiring only a single numerical reservoir routing system implementation. In contrast, the Variational hyetograph proves advantageous when evaluating multiple configurations, enabling analytical solutions for the reservoir routing system and reducing computational demands. Another notable result obtained is the strong performance of the BLUE hyetograph, which accurately estimated maximum outflows using only peak values from the mean annual maxima series. This performance eliminates the need for complete flow time series or IDF curve parameters, making the BLUE hyetograph particularly attractive for gauged basins but limiting its applicability in data-scarce regions.

425 In addition, a critical finding emerged that all design hyetographs consistently underestimated maximum storable volumes compared to continuous simulations. This finding highlights a fundamental shortcoming in event-based design methods, thus the assumption that the full storage volume is available at the beginning of the event may not always hold. Continuous time-series routing demonstrated that accounting for the cumulative effects of antecedent conditions constrains available storage more realistically. Therefore, since antecedent storage from prior events can significantly reduce available flood storage, studies should account for this, otherwise it can lead to under-designed flood control infrastructure. However, these results are sensitive to the rainfall time series available and assuming a single set of basin characteristics may not fully reflect the complexity of real-world watersheds. Future research should explore how these discrepancies evolve under varying upstream basin parameters, such as basin Lag time and rainfall time series, and assess the applicability of these findings. Expanding the scope to include additional case studies would further enhance the robustness of these results.

430 Finally, the observed differences in peak reduction estimate highlight that it is highly sensitive to the choice of input hyetograph. Therefore, the selection of a suitable design hyetograph is critical to ensure reliable performance estimates for

accurately capturing reservoir attenuation behaviour and informing sound design decisions. Considering that the peak reduction effect is often considered a proxy of the efficiency of the reservoir, uncorrected estimates may lead to unrealistic reservoir configuration performances. This behaviour can be further exacerbated when comparing different reservoir configurations,

440

To conclude, while the analysed case studies provide valuable insights, the findings are context-specific and not universally generalisable. Although the case studies cover a wide range of complexities, they do not represent the full diversity of catchment behaviours. Therefore, while this study offers a preliminary yet meaningful contribution to understanding the influence of design hyetograph selection, further research is needed to fully generalise the conclusions across broader hydrological contexts.

445

### Author contribution

**D. Pirone:** Conceptualization, Data curation, Formal analysis, Investigation, Methodology, Software, Validation, Visualization, Writing – original draft preparation, Writing – review & editing. **A. D’Aniello:** Validation, Writing – original draft preparation, Writing – review & editing. **L. Cimorelli:** Writing – review & editing. **D. Pianese:** Conceptualization, Funding acquisition, Methodology, Supervision, Writing – original draft preparation, Writing – review & editing.

450

### Competing interests

The authors declare that they have no conflict of interest.

### Acknowledgements

The authors gratefully acknowledge Eng. Mauro Biafore and Matteo Gentilella from the “Centro Funzionale e Multirischi” of the Campania Region Department of Civil Protection (Naples, Italy) for providing access to rainfall data from their monitoring rain gauge network. The authors also thank Eng. Marcello Nicodemo from “Consorzio di Bonifica Velia” for sharing the data related to the San Giovanni Dam.

455

### References

Alfieri, L., Laio, F., and Claps, P.: A simulation experiment for optimal design hyetograph selection, *Hydrol. Process.*, 22, 813–820, 2008.

Aureli, F., Prost, F., Mignosa, P., and Tomirotti, M.: Validation of Synthetic Design Hydrographs through 2D hydrodynamic modelling, *J. Hydrol.*, 622, 129727, 2023.

460



- Balistrocchi, M., Grossi, G., and Bacchi, B.: Deriving a practical analytical-probabilistic method to size flood routing reservoirs, *Adv. Water Resour.*, 62, 37–46, 2013.
- 465 Cipollini, S., Fiori, A., and Volpi, E.: A new physically based index to quantify the impact of multiple reservoirs on flood frequency at the catchment scale based on the concept of equivalent reservoir, *Water Resour. Res.*, 58, e2021WR031470, 2022.
- Cramer, F., Shephard, G. E., and Heron, P. J.: The misuse of colour in science communication, *Nat. Commun.*, 11, 5444, <https://doi.org/10.1038/s41467-020-19160-7>, 2020.
- 470 Cristiano, E., ten Veldhuis, M. C., and Van de Giesen, N.: Spatial and temporal variability of rainfall and their effects on hydrological response in urban areas – a review, *Hydrol. Earth Syst. Sci.*, 21, 3859–3878, 2017.
- Dimas, P., Sakki, G. K., Kossieris, P., Tsoukalas, I., Efstratiadis, A., Makropoulos, C., and Pipilli, K.: Establishing a Strategic Blueprint for the Design and Evaluation of Flood Control Infrastructure in Extensive Watersheds, *Water Resour. Manag.*, 1–28, 2025.
- 475 Evangelista, G., Ganora, D., Mazzoglio, P., Pianigiani, F., and Claps, P.: Flood Attenuation Potential of Italian Dams: Sensitivity on Geomorphic and Climatological Factors, *Water Resour. Manag.*, 37, 6165–6181, 2023.
- Evangelista, G., Mazzoglio, P., Ganora, D., Pianigiani, F., and Claps, P.: Features of the Italian Large Dams and their upstream catchments, *Earth Syst. Sci. Data Discuss.*, 1–23, <https://doi.org/10.5194/essd-2024-170>, 2024.
- Fischer, S., Dallan, E., Fiori, A., Grimaldi, S., Kochanek, K., Prieto, C., and Volpi, E.: Hydrological design in the HELPING decade – inspiring the community to innovate the hydrological design concept, *Hydrol. Sci. J.*, 1–15, 2025.
- 480 Grimaldi, S., Volpi, E., Langousis, A., Papalexiou, S. M., De Luca, D. L., Piscopia, R., and Petroselli, A.: Continuous hydrologic modelling for small and ungauged basins: A comparison of eight rainfall models for sub-daily runoff simulations, *J. Hydrol.*, 610, 127866, 2022.
- Keifer, C. J. and Chu, H. H.: Synthetic storm pattern for drainage design, *J. Hydraul. Div. ASCE*, 83, 1332-1, 1957.
- 485 Lempérière, F.: Dams and floods, *Engineering*, 3, 144–149, 2017.
- Manfreda, S., Miglino, D., and Albertini, C.: Impact of detention dams on the probability distribution of floods, *Hydrol. Earth Syst. Sci.*, 25, 4231–4242, <https://doi.org/10.5194/hess-25-4231-2021>, 2021.
- Mediero, L., Jiménez-Álvarez, A., and Garrote, L.: Design flood hydrographs from the relationship between flood peak and volume, *Hydrol. Earth Syst. Sci.*, 14, 2495–2505, 2010.
- 490 Merz, B., Basso, S., Fischer, S., Lun, D., Blöschl, G., Merz, R., and Schumann, A.: Understanding heavy tails of flood peak distributions, *Water Resour. Res.*, 58, e2021WR030506, 2022.
- Michailidi, E. M. and Bacchi, B.: Dealing with uncertainty in the probability of overtopping of a flood mitigation dam, *Hydrol. Earth Syst. Sci.*, 21, 2497–2507, 2017.
- Morbidelli, R., Flammini, A., Echeta, O., Albano, R., Anzolin, G., Zumer, D., and Saltalippi, C.: A reassessment of the history of the temporal resolution of rainfall data at the global scale, *J. Hydrol.*, 654, 132841, 2025.
- 495



- Peleg, N., Wright, D. B., Fowler, H. J., Leitão, J. P., Sharma, A., and Marra, F.: A simple and robust approach for adapting design storms to assess climate-induced changes in flash flood hazard, *Adv. Water Resour.*, 193, 104823, 2024.
- Pianese, D. and Rossi, F.: Curve di possibilità di laminazione delle piene, *Giornale del Genio Civile*, 4–6, 131–148, 1986.
- 500 Pirone, D., Cimorelli, L., and Pianese, D.: The effect of flood-mitigation reservoir configuration on peak-discharge reduction during preliminary design, *J. Hydrol. Reg. Stud.*, 52, 101676, 2024.
- Pirone, D., Cimorelli, L., D’Aniello, A., and Pianese, D.: A novel Generalised Semi-Analytical Approach for flood control reservoir design, *Water Resour. Res.*, 61, e2024WR039368, 2025.
- Requena, A. I., Mediero, L., and Garrote, L.: A bivariate return period based on copulas for hydrologic dam design: accounting for reservoir routing in risk estimation, *Hydrol. Earth Syst. Sci.*, 17, 3023–3038, 2013.
- 505 Rossi, F. and Villani, P.: Flood evaluation in Campania Region (in Italian), GNDICI-CNR 1470, 1995.
- Sultan, D., Tsunekawa, A., Tsubo, M., Haregeweyn, N., Adgo, E., Meshesha, D. T., and Setargie, T. A.: Evaluation of lag time and time of concentration estimation methods in small tropical watersheds in Ethiopia, *J. Hydrol. Reg. Stud.*, 40, 101025, 2022.
- Veneziano, D. and Villani, P.: Best linear unbiased design hyetograph, *Water Resour. Res.*, 35, 2725–2738, 1999.
- 510 Volpi, E., Di Lazzaro, M., Bertola, M., Viglione, A., and Fiori, A.: Reservoir effects on flood peak discharge at the catchment scale, *Water Resour. Res.*, 54, 9623–9636, 2018.